Walisongo Journal of Chemistry
Walisongo Journal of Chemistry Vol. 9 Issue 1 (2026), 127-138
ISSN: 2621-5985 (online); 2549-385X (print)
DOI: https://doi.org/10.21580/wjc.v9i1.31931

EFFICIENT CONVERSION OF FURFURYL ALCOHOL TO ETHYL LEVULINATE AND FURFURYL ETHYL ETHER USING COPPER(II) TUNGSTATE CATALYSTS

Husni Wahyu Wijaya[1,2]*, Rima Prastianti Putri[1], Ubed Sonai Fahruddin Arrozi[1]

[1]Department of Chemistry, Faculty of Mathematics and Natural Sciences, Universitas Negeri Malang, Malang 65145, Indonesia
[2]Centre of Advanced Material for Renewable Energy (CAMRY), Universitas Negeri Malang, Malang 65145, Indonesia

*Corresponding author: husni.wahyu.fmipa@um.ac.id

Abstract

Furfuryl alcohol (FFA), a biomass-derived platform compound widely used in polymer synthesis, has considerable potential as a precursor for producing furfuryl ethyl ether (FEE) and ethyl levulinate (EL), which are high-value industrial solvents and fuel additives. Their commercial production requires an active, stable, and inexpensive catalyst. In this study, $CuWO_4$ catalysts calcined at different temperatures ($CuWO_4$-TC, $CuWO_4$-350, $CuWO_4$-500, and $CuWO_4$-650) were synthesized and structurally characterized using powder XRD, FTIR, and SEM-EDX. The catalytic performance of these catalysts in FFA alcoholysis using ethanol as the hydrogen donor was systematically investigated, and the products were analyzed using GC-FID and GC-MS. Among the catalysts, $CuWO_4$-TC exhibited 100% FFA conversion and a 99% EL yield at 160°C for 6 h. The catalytic activity of $CuWO_4$-350 was significantly influenced by temperature and reaction time, with 100% FFA conversion, 2% FEE yield, and 98% EL yield achieved at 180°C for 6 h. These results demonstrate the high efficiency of $CuWO_4$ catalysts for the selective conversion of FFA, offering a promising route for sustainable biomass valorization.

Keywords: *Alcoholysis; Ethyl levulinate; Furfuryl alcohol; Copper tungstate catalyst; Furfuryl ethyl ether*

Introduction

Chemical processes that utilize renewable feedstocks and follow green chemistry principles are recognized as key strategies for reducing dependence on fossil fuels and supporting sustainable industrial development [1], [2]. Furfuryl alcohol (FFA), produced through the hydrogenation of furfural (FFR) derived from lignocellulosic biomass [3], is among the most promising biomass-derived molecules. Owing to its versatile chemical structure, FFA can be converted into several valuable products, including furfuryl ethyl ether (FEE) [4], [5], [6] and ethyl levulinate (EL) [7], [8], [9]. These compounds are of great interest because they possess high octane numbers and favorable physicochemical properties, and they can serve as fuel additives to enhance fuel quality and combustion efficiency [10], [11], [12], [13], [14].

Consequently, the development of efficient methods for converting renewable biomass-derived intermediates into EL represents a critical research focus at the intersection of sustainable chemistry, energy security, and low-carbon fuel technology.

EL is typically synthesized through the alcoholysis of FFA in the presence of acid catalysts to achieve high conversion and selectivity [15]. Numerous homogeneous acid catalysts, including HF, HCl, H_3PO_4, and H_2SO_4, have been employed for this transformation [5], [16]. Although these catalysts are effective, they have substantial drawbacks, including corrosivity, difficulties in product separation and catalyst recovery, and the generation of undesirable waste. To address these limitations, research has increasingly focused on heterogeneous acid catalysts, which offer advantages in separation, reusability, and reduced environmental impact [5], [17]. Several heterogeneous acid catalysts, such as SiO_2–Al_2O_3 [18], kaolinite [19], montmorillonite K10 [20], and $VOSO_4$@MOF-808 [21], have shown promising catalytic performance. However, many of these systems still require large catalyst quantities, elevated pressures, or additional N_2 gas, thereby increasing process complexity and cost. These issues underscore the continuing need for cost-effective, stable, and efficient heterogeneous catalysts capable of promoting FFA alcoholysis under milder and more practical conditions.

Copper tungstate ($CuWO_4$) is a heterogeneous catalyst recognized for its high stability, favorable catalytic properties, and simple and rapid preparation [22]. To date, most research has focused on the application of $CuWO_4$ in photocatalytic reactions [23], [24], whereas its potential in biomass conversion, particularly for the transformation of FFA into EL, remains unexplored. Previous studies on $CuO/WO_3(x)$–Al_2O_3 catalysts have shown that Cu^{2+} acts as a Lewis acid site, while WO_3 provides both Lewis and Brønsted acidity, thereby enhancing catalytic activity [25]. These findings suggest that the Cu^{2+} and WO_4^{2-} sites in $CuWO_4$ may provide the necessary acidity to catalyze FFA alcoholysis. However, $CuWO_4$ has not been systematically investigated for this reaction, indicating a gap in the development of improved heterogeneous catalysts for biomass conversion, particularly in the alcoholysis of FFA to EL.

This study is among the first to examine $CuWO_4$ as a catalyst for converting FFA into EL. By evaluating this heterogeneous catalytic reaction, we aim to advance the understanding of tungstate-based materials for biomass conversion and encourage the development of more sustainable catalytic approaches. If effective, $CuWO_4$ could offer a simple, stable, and cost-effective alternative to current catalysts, supporting renewable chemical production and cleaner fuel additives. This study is intended to contribute to both the scientific understanding and practical application of heterogeneous catalysis for sustainable biomass utilization.

Experimental section

Materials

The materials used in this study were copper(II) nitrate trihydrate ($Cu(NO_3)_2{\cdot}3H_2O$, p.a., Merck), sodium tungstate dihydrate ($Na_2WO_4{\cdot}2H_2O$, p.a., Merck), polyethylene glycol 4000 (PEG 4000, for synthesis, Sigma-Aldrich), furfuryl alcohol ($C_5H_6O_2$, for synthesis, Sigma-Aldrich), ethanol (CH_3CH_2OH, p.a., Merck), naphthalene, and deionized water (DI water).

Procedure

Catalyst Preparation

$CuWO_4$ was synthesized using the coprecipitation method following procedures reported in previous studies [26]. PEG 4000 surfactant, 1.5 mmol, was added to a 5 mmol Na_2WO_4 solution in 50 mL of DI water. Separately, a 5 mmol $Cu(NO_3)_2$ solution was prepared using the same solvent. The Na_2WO_4 solution was gradually added to the $Cu(NO_3)_2$ solution while being heated at 70°C for 4 h. The precipitate was then filtered, washed, and dried at 80°C for 4 h. For comparison, the

obtained solids were treated under different calcination conditions: without calcination, 350°C, 500°C, and 650°C. The samples were labeled $CuWO_4$-TC, $CuWO_4$-350, $CuWO_4$-500, and $CuWO_4$-650, respectively.

Catalyst Characterization

The structure of the materials was analyzed by XRD (Rigaku Miniflex 600) using Cu Kα radiation (λ = 1.5409 Å) over a 2θ range of 5°–90°. FTIR spectroscopy (Bruker Alpha; ZnSe beam splitter) was used to identify functional groups from infrared spectra in the range of 4000–500 cm^{-1}. The surface morphology of the materials and the distribution of their constituent elements were analyzed using SEM-EDX (FEI Inspect-S50) at an acceleration voltage of 20.00 kV.

Alcoholysis of Furfuryl Alcohol

The catalytic tests were carried out in a batch reactor. For each reaction, 3 mL of ethanol, 1 mmol of FFA, and 0.05 g of $CuWO_4$-X were added to the reactor (autoclave). All reactions were conducted at 160°C and stirred at 800 rpm for 6 h. The products were then analyzed using GC-FID (PerkinElmer) and GC-MS (Agilent).

FFA conversion and product yields were determined by GC-FID based on peak area using Equations (1) and (2). The oven temperature was programmed from 75 to 200°C at 10°C/min using a capillary column (SGE Analytical Science). GC-MS was used to identify the product compounds. The analysis was performed by the Forensic Laboratory Center of the Indonesian National Police (POLRI) using the same heating program and a 19091S-433 (HP-5MS) column.

$$\%\ \text{Conversion} = 1 - \frac{\text{FFA area peak}}{\text{Total area peak}} \times 100\% \quad (1)$$

$$\%\ \text{Yield} = 1 - \frac{\text{Product area peak}}{\text{Total product area peak}} \times 100\% \quad (2)$$

Results and Discussion

Characterization of the As-Prepared Copper(II) Tungstate Catalysts

The agreement between the 2θ diffraction pattern of the synthesized $CuWO_4$ and the reference COD No. 1008036 (see Figure 1a) confirms the formation of the $CuWO_4$ phase with a triclinic structure and P1 space group. The peaks of $CuWO_4$-TC and $CuWO_4$-350 were low in intensity and overlapped, whereas those of $CuWO_4$-500 became more distinct and those of $CuWO_4$-650 became sharper. This variation was influenced by calcination temperature, which enhanced crystallinity [27].

Several researchers have reported that the crystalline phase of $CuWO_4$ begins to form at temperatures of ≥500°C, whereas other phases, such as $CuWO_4{\cdot}2H_2O$, form at lower temperatures [24], [28], [29]. The diffraction pattern of $CuWO_4$-350 showed broad, low-intensity peaks, indicating its amorphous character [30].

The structural agreement between the $CuWO_4$-500 catalyst and reference COD No. 1008036 was further evaluated by Rietveld refinement, as shown in Figure 1b. The refinement was performed using Rietica software, yielding Rp = 10.13%, Rwp = 11.50%, and GOF = 1.42. These results indicate that $CuWO_4$-500 has a triclinic structure belonging to the P1 space group.

Analysis of the IR spectra revealed similarities among the as-synthesized samples, as shown in Figure 2. The broad band observed in the 3400–2880 cm^{-1} region indicates the presence of symmetric and asymmetric stretching vibrations of water molecules adsorbed on the $CuWO_4$ surface. This finding is supported by bands at 1632 and 1467–1240 cm^{-1}, which are associated with bending vibrations of hydroxyl groups (-OH) and free hydrogen radicals [30], [31]. Furthermore, the strong bands at 1097–910 cm^{-1} are attributed to symmetric O-W-O stretching vibrations [29], [32], [33], while the band in the 800–700 cm^{-1} range corresponds to asymmetric O-W-O stretching vibrations [33]. The XRD diffractogram showed that higher calcination temperatures increased the crystallinity of $CuWO_4$ by reducing the amount of adsorbed water on the tungsten oxide surface. This trend was confirmed by the FTIR spectra, which showed a decrease

in the intensity of the band in the 3400–2880 cm^{-1} region.

SEM-EDX mapping analysis was conducted on samples before and after reaction to observe differences in morphology, elemental distribution, and elemental composition. The results (see Figure 3a,b) indicate that both samples had irregular shapes. Before the reaction, the $CuWO_4$-350 surface exhibited relatively fine and dispersed grains; after the reaction, these grains evolved into agglomerates with smoother surfaces. In the EDX analysis, carbon (C) was detected from the sample holder and was therefore excluded because it is not part of the $CuWO_4$ structure. The elemental contents detected in $CuWO_4$-350 were copper (Cu) at 11.92 wt%, tungsten (W) at 15.55 wt%, and oxygen (O) at 14.39 wt%. Notably, the oxygen content before the reaction was lower than that after the reaction (18.04 wt%). This increase in oxygen content suggests changes in surface composition due to oxide formation [34].

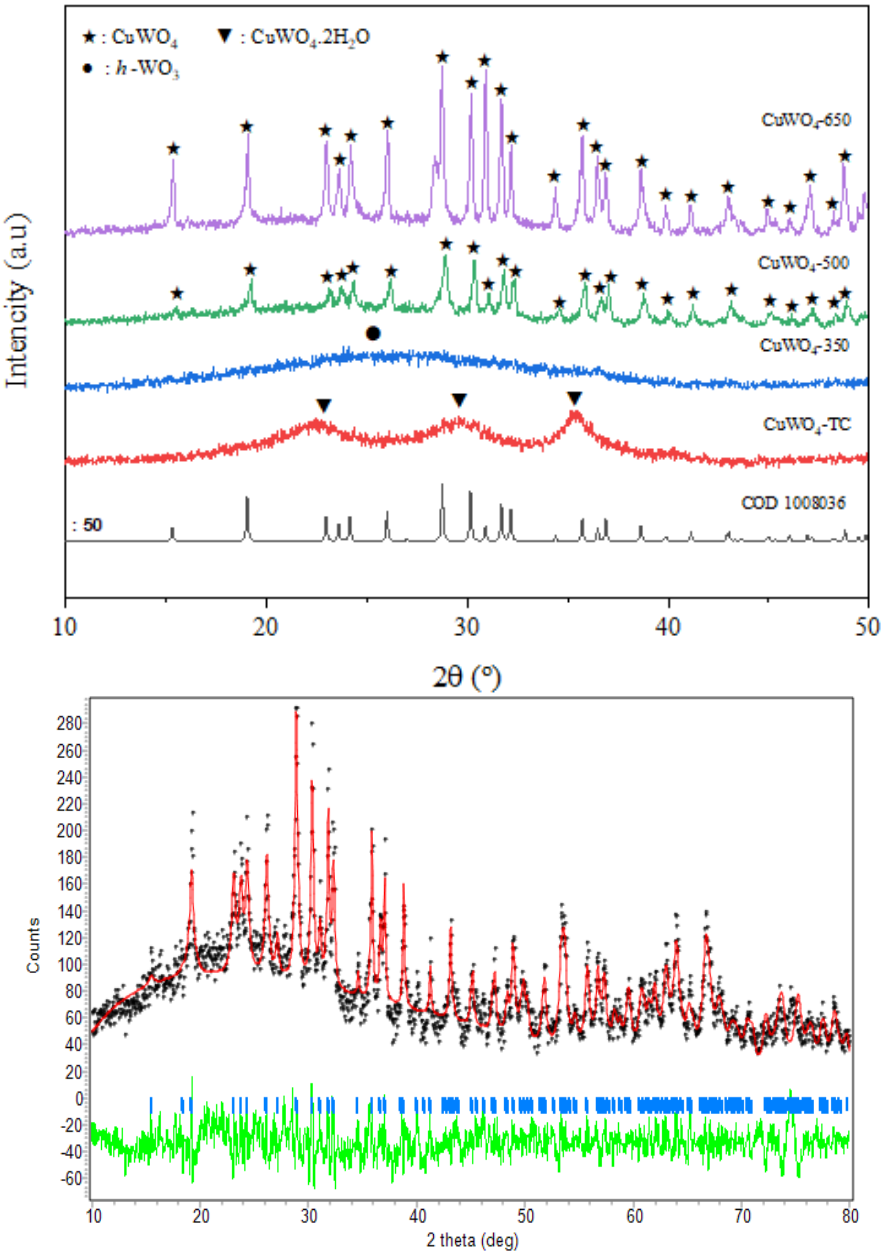

Figure 1. (a) XRD patterns of synthesized $CuWO_4$ and (b) Rietveld refinement results of $CuWO_4$-500.

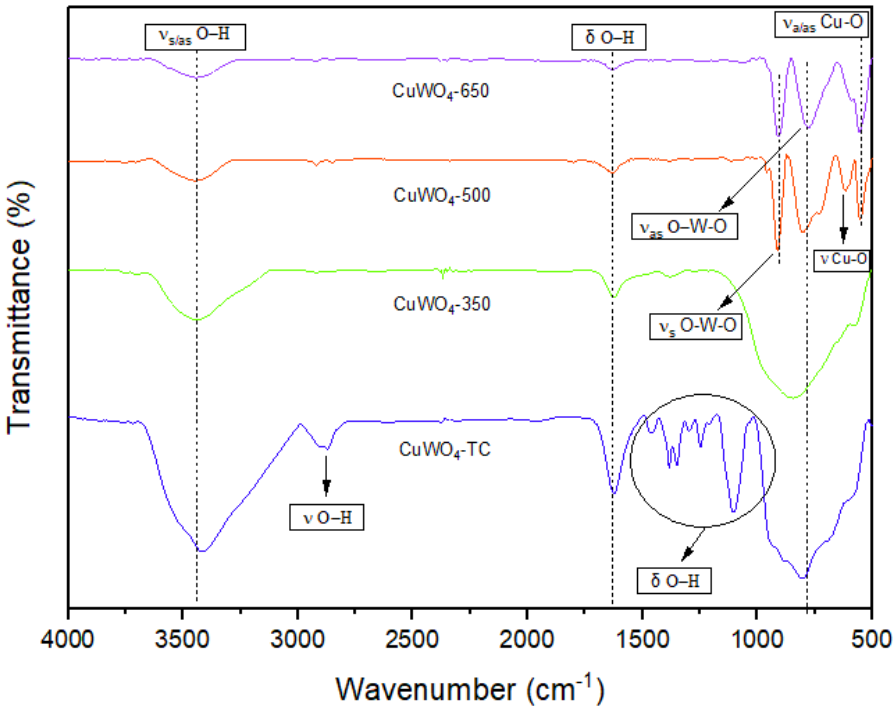

Figure 2. FTIR spectra of $CuWO_4$ at various calcination temperatures.

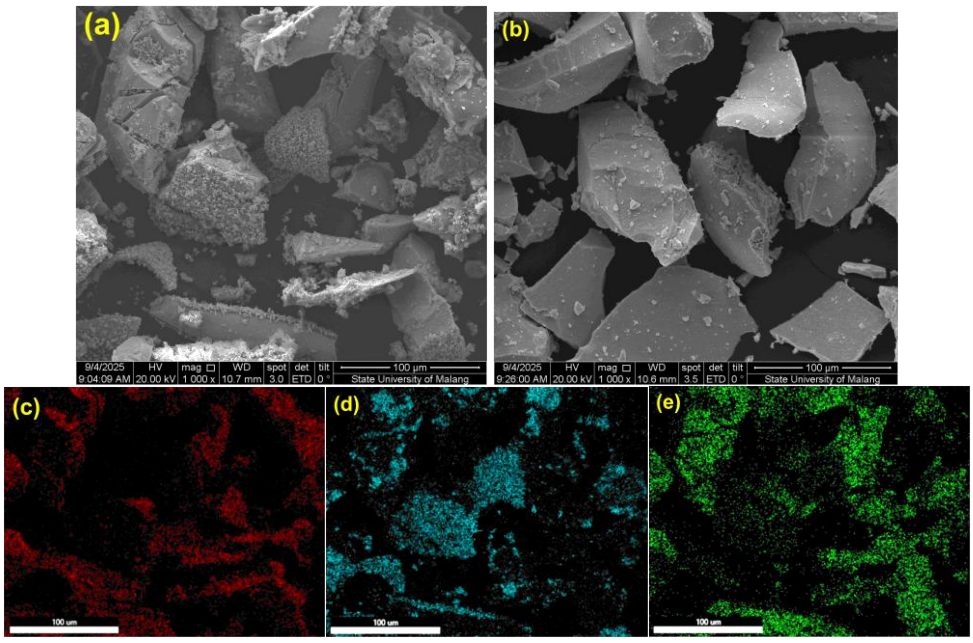

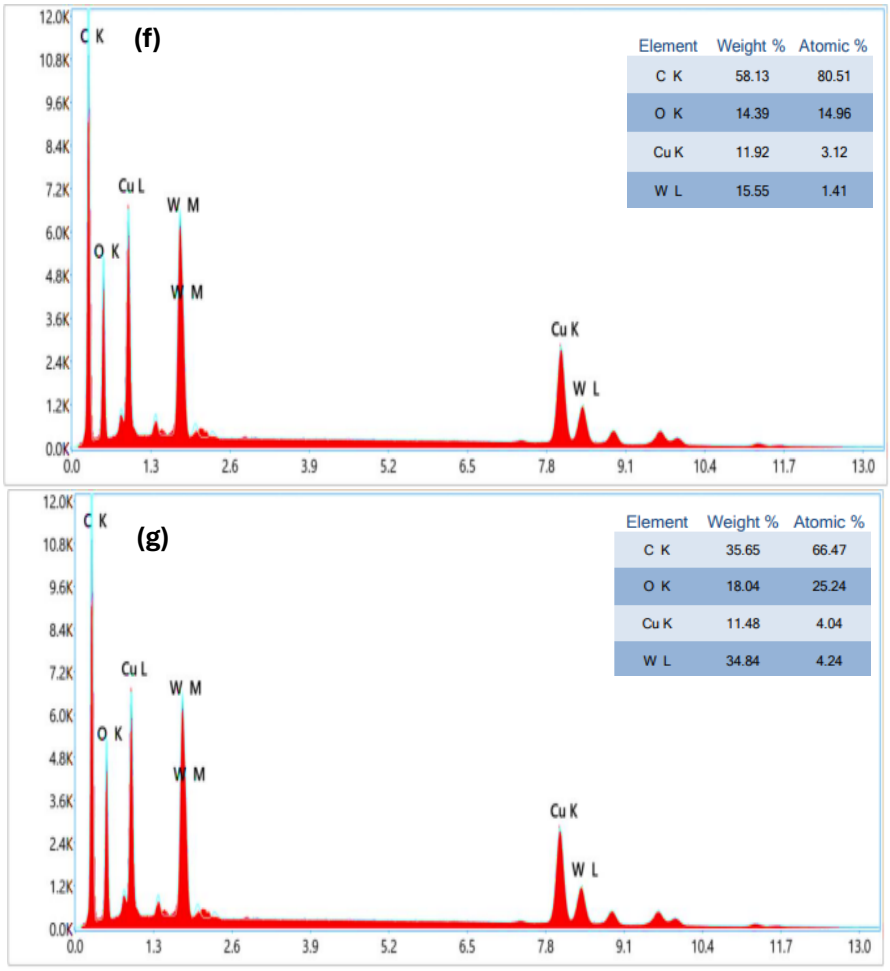

Figure 3. SEM images of $CuWO_4$-350 (a) before and (b) after the reaction; SEM-EDX mapping showing the atomic distribution of (c) O, (d) Cu, and (e) W in $CuWO_4$-350; particle size distribution of $CuWO_4$-350 (f) before and (g) after the reaction.

Alcoholysis of FFA

The effect of catalyst variation on the alcoholysis of FFA is shown in Table 1. The catalytic activities of the precursor salts $Na_2WO_4{\cdot}2H_2O$ and $Cu(NO_3)_2{\cdot}3H_2O$ are presented in Table 1 (Entries 1 and 2). The catalytic performance of these precursors in forming EL was lower than that of the $CuWO_4$ catalysts. In contrast, all $CuWO_4$-X catalysts achieved conversion rates of up to 100%, except for $CuWO_4$-650. The decreased conversion observed for $CuWO_4$-650 was likely due to a reduction in acid sites caused by calcination, which removes hydroxyl groups (-OH) from the catalyst surface. This loss decreases the number of Brønsted acid sites, which are essential for facilitating alcoholysis reactions [35], [36], [37]. Notably, the $CuWO_4$-TC catalyst achieved 100% FFA conversion and a 99% EL yield, whereas the $CuWO_4$-350 catalyst produced a 29% EL yield with minimal side reactions, indicating a favorable balance between activity and selectivity. In addition, the $Fe_2(WO_4)_3$ catalyst achieved 97% FFA conversion and a 52% EL yield. This result suggests that Fe-based tungstate also possesses active acidic sites for the reaction, although its selectivity is lower. The differences in catalytic performance among the catalyst variants can be attributed to variations in acidity, crystallinity, and crystal phase.

Table 1. Catalytic alcoholysis reaction between furfuryl alcohol and ethanol

Entry	Catalyst	Conversion (%)	Yield (%)		
			FEE	EL	Unknown
1	$Na_2WO_4.2H_2O$	18	17	1	0
2	$Cu(NO_3)_2.3H_2O$	59	58	1	0
3	$CuWO_4$-TC	100	1	99	0
4	$CuWO_4$-350	100	69	29	2
5	$CuWO_4$-500	100	86	12	2
6	$CuWO_4$-650	62	53	9	0
7	$Fe_2(WO_4)_3$	97	45	52	0

Reaction conditions: 1 mmol of FFA; 3 mL of ethanol; 0.05 g of catalyst; 160°C; 6 h.

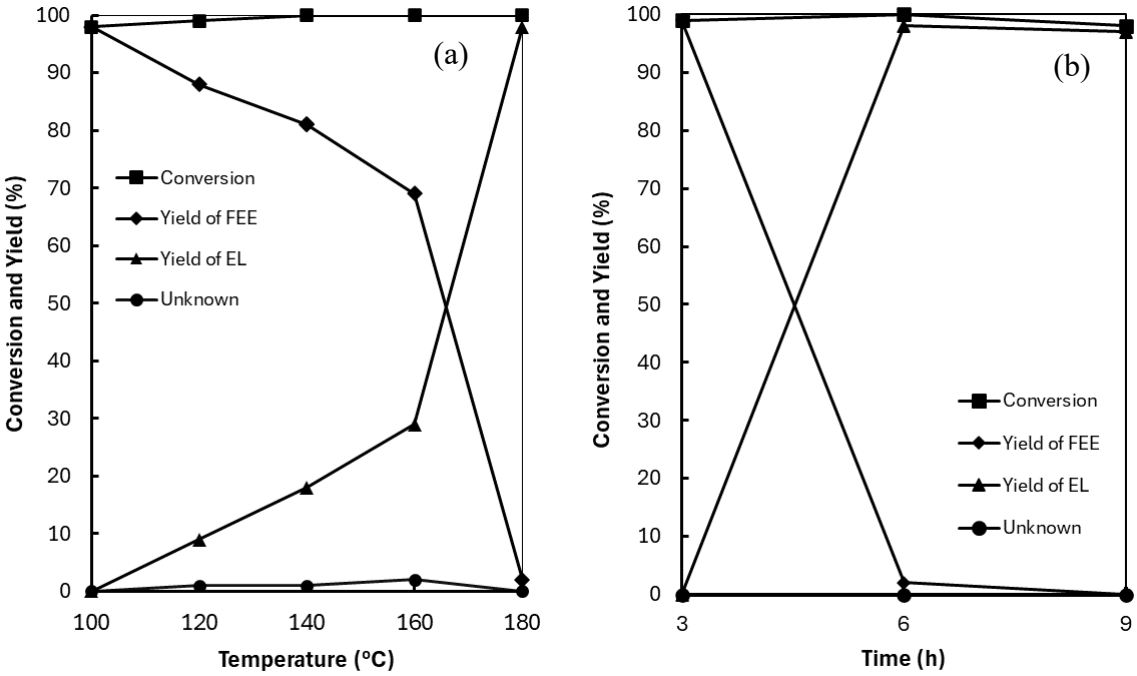

Figure 4. (a) Effect of temperature on the alcoholysis of FFA in ethanol. Reaction conditions: 1 mmol of FFA; 3 mL of ethanol; 0.05 g of $CuWO_4$-350; 6 h. (b) Effect of reaction time on the alcoholysis of FFA in ethanol. Reaction conditions: 1 mmol of FFA; 3 mL of ethanol; 0.05 g of $CuWO_4$-350; 180°C.

The effect of temperature was investigated over the range of 100–180°C, with the results shown in Figure 4a. All reaction temperatures resulted in high FFA conversion. Increasing the reaction temperature enhanced the conversion of FEE to EL. At 100°C, EL had not yet formed, and FFA was converted into FEE. EL formation began at 120°C with a 9% yield and continued to increase, reaching 98% at 180°C. The amounts of unidentified products formed at all temperatures were very low and can therefore be disregarded. Thus, the intermediate FEE was produced in greater amounts at lower temperatures, as these conditions were insufficient to convert it into EL.

The influence of reaction time was examined at 3, 6, and 9 h, with the results presented in Figure 4b. Within the first 3 h, 99% FFA conversion was achieved, yielding 99% of the intermediate FEE and less than 1% EL. After 6 h, FFA conversion reached 100%, accompanied by substantial changes

in product yields: 98% EL and 2% FEE. When the reaction time was extended to 9 h, FFA conversion and EL yield decreased to 98% and 97%, respectively, while the FEE yield dropped to nearly 0%. In addition, the formation of unidentified products increased slightly. However, the amounts of these unidentified products formed at all reaction times were very low and can be considered negligible. Thus, increasing the reaction time decreased the FEE yield and initially increased the EL yield. When the reaction time exceeded the optimal condition, the EL yield decreased because EL was converted into other byproducts.

Alcoholysis Reaction Route

In this study, the alcoholysis reaction of FFA was investigated using ethanol as the solvent, with FEE identified as an intermediate. In this reaction, ethanol acts as a nucleophile, attacking the electrophilic center of the substrate (de Jong et al., 2012). Ethanol may also participate in proton-transfer steps through its -OH group. In the initial stage, FFA reacts with ethanol to form FEE through direct etherification (Wang et al., 2025). Subsequently, FEE undergoes furan-ring opening, yielding EL as the final product. According to the literature, FEE formation is a key step in the conversion of FFA into EL (Wang et al., 2014; Hu et al., 2022b). The formation of FEE as an intermediate is influenced by the -OH group of the substrate, which can act as a leaving group after protonation. To examine the role of the -OH group in the reaction route, several substrates, including FFR and tetrahydrofurfuryl alcohol (THFA), were reacted with ethanol. The results are shown in Table 2. The formation of EL from FFA proceeds through FEE, which serves as a key precursor for the ring-opening and rearrangement reactions. By contrast, THFA, which lacks a conjugated furan ring, did not form FEE or EL. Meanwhile, FFR, which lacks the hydroxyl group required for ether formation, did not produce FEE or EL under the same reaction conditions. The proposed reaction route for EL formation in this study is illustrated in Figure 5.

The results indicate that the presence of the -OH group determines the initial stage of FEE formation because it can act as a leaving group after protonation. This -OH group plays an important role in facilitating FEE formation and is more effective in unsaturated substrates such as FFA. FEE subsequently acts as an important intermediate in EL formation through hydrolysis and rearrangement under acidic conditions (González Maldonado *et al.*, 2012; Hu *et al.*, 2022c). Without the -OH group, EL formation occurs more slowly because FEE is not formed through the same pathway.

Table 2. Effect of substrate variation on alcoholysis in ethanol

Entry	Substrate	Conversion (%)	Yield (%)		
			FEE	EL	Unknown
1	FFR	100	0	0	0
2	THFA	0	0	0	0

Reaction conditions: 1 mmol of substrate; 3 mL of ethanol; 0.05 g of $CuWO_4$-350 catalyst; 160°C; 6 h.

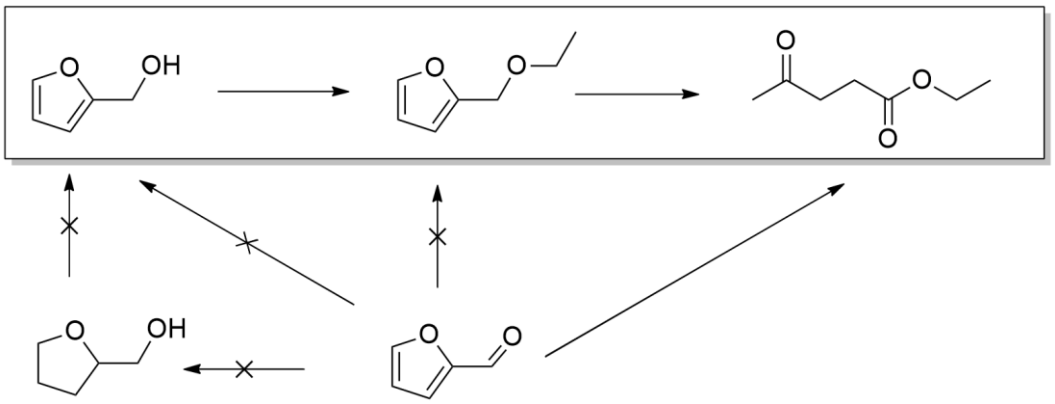

Figure 5. Proposed reaction route for the alcoholysis of furfuryl alcohol to ethyl levulinate with ethanol.

Conclusion

$CuWO_4$, prepared by coprecipitation, was successfully applied as a catalyst in the alcoholysis of FFA. Among the tested catalysts, $CuWO_4$-TC achieved complete FFA conversion and a 99% EL yield at 160°C for 6 h. Further evaluation of $CuWO_4$-350 showed that reaction temperature and time significantly influenced catalytic efficiency. At 180°C for 6 h, $CuWO_4$-350 achieved complete FFA conversion, yielding 2% FEE and 98% EL. Further research should address catalyst stability, reusability, reaction mechanisms, and process scale-up to evaluate the industrial applicability of this catalytic system.

Acknowledgement

This work was supported by a Non-Budgeting (Non-APBN) Research Grant from the Institute of Research and Community Engagement, Universitas Negeri Malang, under the Bachelor Thesis Scheme, contract number 24.2.632/UN32.14.1/LT/2025.

References

[1] Y. Jing, Y. Guo, Q. Xia, X. Liu, and Y. Wang, "Catalytic Production of Value-Added Chemicals and Liquid Fuels from Lignocellulosic Biomass," *Chem*, vol. 5, no. 10, pp. 2520–2546, Oct. 2019, doi: 10.1016/j.chempr.2019.05.022.

[2] V. K. Vaithyanathan, B. Goyette, and R. Rajagopal, "A critical review of the transformation of biomass into commodity chemicals: Prominence of pretreatments," *Environ. Challenges*, vol. 11, no. January, p. 100700, 2023, doi: 10.1016/j.envc.2023.100700.

[3] X. Guo, H. Wu, P. Wu, M. He, and Y. Guan, "Efficient synthesis of bioetheric fuel additive by combining the reductive and direct etherification of furfural in one-pot over Pd nanoparticles deposited on zeolites," *Green Energy Environ.*, vol. 8, no. 2, pp. 519–529, 2023, doi: 10.1016/j.gee.2021.07.001.

[4] A. Hu, H. Wang, and J. Ding, "Novel Sulfonic Acid Polystyrene Microspheres for Alcoholysis of Furfuryl Alcohol to Ethyl Levulinate," *Catal. Letters*, vol. 152, no. 10, pp. 3158–3167, 2022, doi: 10.1007/s10562-021-03881-5.

[5] A. Hu, H. Wang, and J. Ding, "Alcoholysis of Furfuryl Alcohol to Ethyl Levulinate Catalyzed by a Deep Eutectic Solvent," *ACS Omega*, vol. 7, no. 37, pp. 33192–33198, 2022, doi: 10.1021/acsomega.2c03424.

[6] W. Deng *et al.*, "Catalytic conversion of lignocellulosic biomass into chemicals and fuels," *Green Energy Environ.*, vol. 8, no. 1, pp. 10–114, 2023, doi: 10.1016/j.gee.2022.07.003.

[7] D. Padovan, A. Al-Nayili, and C. Hammond, "Bifunctional Lewis and Brønsted acidic zeolites permit the

continuous production of bio-renewable furanic ethers," *Green Chem.*, vol. 19, no. 12, pp. 2846–2854, 2017, doi: 10.1039/c7gc00160f.

[8] N. L. Mulik, P. S. Niphadkar, and V. V. Bokade, "Synthesis of ethyl furfuryl ether (potential biofuel) by etherification of furfuryl alcohol with ethanol over heterogenized reusable H1Cs2PW12O40 catalyst," *Res. Chem. Intermed.*, vol. 46, no. 4, pp. 2309–2325, 2020, doi: 10.1007/s11164-020-04093-z.

[9] A. Hu, H. Wang, and J. Ding, "Synthesis of ethyl levulinate from furfuryl alcohol using waste yeast/sulfonic acid heterogeneous catalyst system," *Chem. Pap.*, vol. 76, no. 12, pp. 7535–7544, 2022, doi: 10.1007/s11696-022-02405-8.

[10] Y. Bai, Y. Liu, F. Bai, Q. Sun, L. Li, and T. Zhang, "Conversion of furfuryl alcohol to ethyl levulinate in the presence of mesoporous aluminosilicate catalyst," *Open Chem.*, vol. 19, no. 1, pp. 1303–1309, 2021, doi: 10.1515/chem-2021-0121.

[11] Yogita, B. S. Rao, C. Subrahmanyam, and N. Lingaiah, "The selective conversion of furfuryl alcohol to ethyl levulinate over Zr-modified tungstophosphoric acid supported on β-zeolites," *New J. Chem.*, vol. 45, no. 6, pp. 3224–3233, 2021, doi: 10.1039/d0nj05296e.

[12] I. S. Khusnutdinov, A. G. Safiulina, D. N. Safina, and I. N. Goncharova, "The effect of oxygen-containing additives obtained from ethanol on basic properties of diesel fuel," *Renew. Energy*, vol. 240, no. December 2024, p. 122233, 2025, doi: 10.1016/j.renene.2024.122233.

[13] G. M. González Maldonado, R. S. Assary, J. A. Dumesic, and L. A. Curtiss, "Acid-catalyzed conversion of furfuryl alcohol to ethyl levulinate in liquid ethanol," *Energy Environ. Sci.*, vol. 5, no. 10, pp. 8990–8997, 2012, doi: 10.1039/c2ee22486k.

[14] D. Zhao *et al.*, "Effective synthesis of ethyl levulinate via alcoholysis of furfuryl alcohol over simple nickel-titanium dioxide," *Appl. Catal. A Gen.*, vol. 648, no. August, p. 118921, 2022, doi: 10.1016/j.apcata.2022.118921.

[15] M. S. Tiwari, A. B. Gawade, and G. D. Yadav, "Magnetically separable sulfated zirconia as highly active acidic catalysts for selective synthesis of ethyl levulinate from furfuryl alcohol," *Green Chem.*, vol. 19, no. 4, pp. 963–976, 2017, doi: 10.1039/c6gc02466a.

[16] J. P. Lange, W. D. van de Graaf, and R. J. Haan, "Conversion of furfuryl alcohol into ethyl levulinate using solid acid catalysts," *ChemSusChem*, vol. 2, no. 5, pp. 437–441, 2009, doi: 10.1002/cssc.200800216.

[17] H. Gong *et al.*, "Catalytic conversion of levulinic acid or furfural alcohol into ethyl levulinate using a sulfonic acid-functionalized coffee biochar," *Fuel*, vol. 352, no. June, 2023, doi: 10.1016/j.fuel.2023.129059.

[18] Q. Cao, W. Zhang, S. Luo, R. Guo, and D. Xu, "Synthesis of Furanic Ethers from Furfuryl Alcohol for Biofuel Production," *Energy and Fuels*, vol. 35, no. 15, pp. 12725–12733, 2021, doi: 10.1021/acs.energyfuels.1c01061.

[19] T. A. Natsir, T. Hara, N. Ichikuni, and S. Shimazu, "Kaolinite Catalyst for the Production of a Biodiesel-Based Compound from Biomass-Derived Furfuryl Alcohol," *ACS Appl. Energy Mater.*, vol. 1, no. 6, pp. 2460–2463, 2018, doi: 10.1021/acsaem.8b00694.

[20] N. Yamanaka, K. Nishi, K. Yasunaga, and H. Yamada, "Synthesis of ethyl furfuryl ether via etherification of furfuryl alcohol with ethanol over montmorillonite K10," *RSC Adv.*, vol. 14, no. 35, pp. 25221–25226, 2024, doi: 10.1039/d4ra03921a.

[21] U. S. F. Arrozi *et al.*, "Applied Catalysis A , General Etherification of furfuryl alcohol catalyzed by vanadium-modified MOF-808 : Thermocatalysis and UV-assisted thermocatalysis," *Appl. Catal. A, Gen.*, vol. 706, no. July, p. 120472, 2025, doi: 10.1016/j.apcata.2025.120472.

[22] M. R. Pratama *et al.*, "Hydrogenolysis of furfuryl alcohol to 1,2-pentanediol catalyzed by first row transition metal salts," *Commun. Sci. Technol.*, vol. 9, no. 2, pp. 421–429, 2024, doi: 10.21924/cst.9.2.2024.1549.

[23] T. Montini, V. Gombac, A. Hameed, L. Felisari, G. Adami, and P. Fornasiero, "Synthesis, characterization and photocatalytic performance of transition metal tungstates," *Chem. Phys. Lett.*, vol. 498, no. 1–3, pp. 113–119, 2010, doi: 10.1016/j.cplett.2010.08.026.

[24] T. T. My Hang, N. H. Thao Vy, N. T. Hanh, T. D. Pham, and L. T. Hoang Yen, "Facile synthesis of copper tungstate (CuWO4) for novel photocatalytic degradation of tetracycline under visible light," *Sustain. Chem. Pharm.*, vol. 21, no. September 2020, p. 100407, 2021, doi: 10.1016/j.scp.2021.100407.

[25] M. Mafokoane, J. Seguel, R. García, J. N. Díaz de León, C. Sepúlveda, and N. Escalona, "Conversion of levulinic acid using CuO/WO3(x)-Al2O3 catalysts," *Catal. Today*, vol. 367, no. February 2020, pp. 310–319, 2021, doi: 10.1016/j.cattod.2020.02.028.

[26] F. Sedighi, M. Esmaeili-Zare, A. Sobhani-Nasab, and M. Behpour, "Synthesis and characterization of CuWO4 nanoparticle and CuWO4/NiO nanocomposite using co-precipitation method; application in photodegradation of organic dye in water," *J. Mater. Sci. Mater. Electron.*, vol. 29, no. 16, pp. 13737–13745, 2018, doi: 10.1007/s10854-018-9504-3.

[27] F. He, F. Ma, J. Li, T. Li, and G. Li, "Effect of calcination temperature on the structural properties and photocatalytic activities of solvothermal synthesized TiO2 hollow nanoparticles," *Ceram. Int.*, vol. 40, no. 5, pp. 6441–6446, 2014, doi: 10.1016/j.ceramint.2013.11.094.

[28] V. Balasubramanian, S. Kannan, S. T. Nishanthi, G. Sivakumar, and K. Mohanraj, "Elucidate the pseudocapacitive behaviour of CuWO4 electrode synthesized by solid-state reaction," *J. Mater. Sci. Mater. Electron.*, vol. 31, no. 13, pp. 10142–10150, 2020, doi: 10.1007/s10854-020-03559-5.

[29] E. L. S. Souza *et al.*, "Structural evolution, growth mechanism and photoluminescence properties of CuWO4 nanocrystals," *Ultrason. Sonochem.*, vol. 38, pp. 256–270, 2017, doi: 10.1016/j.ultsonch.2017.03.007.

[30] H. Chen and Y. Xu, "Photocatalytic organic degradation over W-rich and Cu-rich CuWO4 under UV and visible light," *RSC Adv.*, vol. 5, no. 11, pp. 8108–8113, 2015, doi: 10.1039/C4RA13952F.

[31] X. Hu *et al.*, "Fabrication of novel CuWO4 nanoparticles (NPs) for photocatalytic degradation of methylene blue in aqueous solution," *SN Appl. Sci.*, vol. 1, no. 1, pp. 1–10, 2019, doi: 10.1007/s42452-018-0113-9.

[32] H. Boudghene Stambouli, F. Guenfoud, A. Benomara, M. Mokhtari, and M. Sönmez-Çelebi, "Synthesis of FeWO4 heterogeneous composite by the sol–gel process: enhanced photocatalytic activity on malachite green," *React. Kinet. Mech. Catal.*, vol. 133, no. 1, pp. 563–578, 2021, doi: 10.1007/s11144-021-01994-x.

[33] D. R. Komatireddy, S. Andem, P. P. Gotipamul, V. V. Rajankumar, and S. Chidambaram, "Harnessing the potential of transition metal tungstates (MWO4, M = Ni, Co, Cu, and Zn) for high-performance asymmetric supercapacitors," *J. Energy Storage*, vol. 100, no. PA, p. 113557, 2024, doi: 10.1016/j.est.2024.113557.

[34] H. Over, "Microscopic insights into the initial oxidation process of single crystalline platinum group metal surfaces: From subsurface oxygen, a ghost species, towards surface oxide," *Surf. Sci. Rep.*, vol. 80, no. 2–3, 2025, doi: 10.1016/j.surfrep.2025.100659.

[35] M. Begala, L. Corda, G. Podda, M. A. Fedrigo, and P. Traldi, "Headspace

solid-phase microextraction gas chromatography/mass spectrometry in the analysis of the aroma constituents of 'Cannonau of Jerzu' wine," *Rapid Commun. Mass Spectrom.*, vol. 16, no. 11, pp. 1086–1091, 2002, doi: 10.1002/rcm.675.

[36] G. Wang, Z. Zhang, and L. Song, "Efficient and selective alcoholysis of furfuryl alcohol to alkyl levulinates catalyzed by double SO3H-functionalized ionic liquids," *Green Chem.*, vol. 16, no. 3, pp. 1436–1443, 2014, doi: 10.1039/c3gc41693c.

[37] W. Zhang, Y. Zhu, H. Xu, M. Gaborieau, J. Huang, and Y. Jiang, "Glucose conversion to 5-hydroxymethylfurfural on zirconia: Tuning surface sites by calcination temperatures," *Catal. Today*, vol. 351, no. October 2018, pp. 133–140, 2020, doi: 10.1016/j.cattod.2018.10.002.